



OPEN

DATA DESCRIPTOR

A comprehensive grain-size database of surface sediments from the Taklamakan Desert

Huiliang Li^{1,2,3}, Xin Gao^{2,3} , Yongcheng Zhao^{2,3}, Jie Zhou^{2,3}, Zihao Hu^{2,3}, Zhuo Chen^{2,3}, Zuowei Yang^{2,3} & Shengyu Li^{2,3}

This study compiles the most comprehensive open-access surface sediment grain-size database (n = 596 samples) spanning the entire Taklamakan Desert, obtained through systematic field sampling and laser diffraction analysis. It provides essential data for understanding the desert formation, evolution, sand sources, and the restoration of aeolian environments. By analyzing key sediment parameters (mean grain size, sorting, skewness, kurtosis) and particle compositions, the dataset reveals sediment transport dynamics and depositional processes critical for understanding desert formation, sand provenance, and aeolian environmental reconstruction. The quantitative characterization of sediment texture and sorting mechanisms provides foundational data for investigating regional dust emissions, wind erosion patterns, and sediment transport capacities. While the primary focus is on the Taklamakan Desert, the methodology and dataset apply to other arid regions, making it a valuable resource for comparative desert studies. It is an indispensable tool for researchers investigating desert landscapes and addressing environmental challenges related to desertification and aeolian processes.

Background & Summary

Over one-third of the global landmass is characterized by arid and semi-arid zones, which are important components of Earth's surface system and affect the global climate, environment, and human survival¹. Environmentally sensitive and fragile deserts and sandy lands, which are common types of aeolian sand deposits in arid and semi-arid regions, are natural laboratories for examining the interactions between the various layers of Earth's surface and human–Earth relationships^{2–4}. Sediment is the material basis for forming and developing aeolian geomorphology: an issue that must be elaborated upon in geomorphological research⁵. The grain size of surface sediments can reflect the transportation and sorting of sand sources by eolian processes⁶, compositional attributes of sediments⁷, vegetation cover status⁸, and proximity to the sand source. Accordingly, we can further analyze the causes and processes of forming different geomorphologies. Therefore, the use of particle size to extract environmental information on sediments has become a hotspot in sedimentology^{7,9–11}.

Grain size is mainly determined by the transport medium, modes of sediment transport, and depositional environment^{12–14}. Grain size parameters (mean grain size, sorting, skewness, and kurtosis) characterize the size of sediment particles. These indicators can measure the energy of the sediment transport medium and transport mode¹⁵. Traditional grain size parameters, while widely used in sediment classification and dynamic process interpretation, are insufficiently sensitive to complex hydrodynamic superposition or multi-source mixed sedimentation. Additionally, the computational discrepancies between different methods can complicate data integration. In recent years, the application of modern grain size parameters has significantly improved the interpretative accuracy of sedimentary dynamics. For instance, the sand-silt-clay percentages can be visually differentiated in fluvial, aeolian, and tidal sedimentary environments through a ternary diagram^{16,17}. By identifying the peak of the grain size distribution, the modal value reflects the differences in transport mechanisms. Grain size end-member modeling (EMMA) is used to analyze provenance and sedimentary dynamics^{18,19}. Furthermore, the U-ratio, by quantifying sorting, distinguishes sedimentary dynamic conditions. The fractal dimension has unique advantages, including comprehensiveness and sensitivity, in reflecting the structural

¹College of Ecology and Environment, Xinjiang University, Urumqi, 830017, China. ²State key Laboratory of Ecological Safety and Sustainable Development in Arid Lands, Xinjiang Institute of Ecology and Geography, Chinese Academy of Sciences, 818 South Beijing Road, Urumqi, 830011, Xinjiang, China. ³University of Chinese Academy of Sciences, Beijing, 100049, China. ✉e-mail: gaoxin@ms.xjb.ac.cn

characteristics of clastic particle size composition²⁰. Previous studies have used grain size analysis methods for the Taklamakan Desert^{7,21}, Badain Jaran Desert²², Kumtagh Sand Sea²³, Namib Desert²⁴, Kalahari Desert^{25,26}, and other sand seas worldwide. Significant progress has occurred, focusing on sand composition, source tracing, and identifying depositional environments in these areas. Lancaster²⁴ showed that sediments in the Namib Desert are composed of well-sorted fine sands and moderately sorted medium sands. Zhang *et al.*²⁷ examined the grain size of dunes in the Tengger Desert, finding that aeolian sands are mainly composed of very fine sand and fine sand: the finer the grain size, the better the sorting. Tsoar²⁸ investigated sediments from the Sinai Desert, finding that the Seif Dunes mainly consist of fine sand with a single peak pattern. The interdune sands of the Kumtag Desert are bimodal in distribution, and interdune sediments are dominated by fine sand, followed by coarse sand, very fine sand, and medium sand²³. Additionally, Gao *et al.*²⁹ used a cellular automaton model to analyze the vertical sorting of particle mixtures under steady unidirectional flow conditions, suggesting that the armor layer should be present in most arid deserts, which may control dune morphodynamics. Van IJendoorn *et al.*³⁰ applied a numerical aeolian sediment-transport model. They observed that the vertical variability in the grain size had a limited effect on the total transport rate. In contrast, horizontal grain size variability affected the total transport rate and grain size composition of the downwind bed.

Many studies have been conducted on the grain sizes of sediments in the Taklamakan Desert^{15,21,31–35}. For example, Chen *et al.*³⁴ showed that the 2–16 μm fractions of the are mainly derived from bedrock. The 32–63 and $>63 \mu\text{m}$ fractions are dominated by regionally sourced material mainly from neighboring mountains (e.g., the Pamir Plateau, Kunlun Mountains, Kuruktag Mountains, Altun Mountains, and Tianshan Mountains). The riverine system is an important additional transport mechanism. Jiang and Yang²¹ analyzed the variation in the average grain size, sorting, and dust fraction content ($<63 \mu\text{m}$) of sediments along the Tarim Desert Road (from Luntai to Minfeng). The results showed that the average particle size was 89–281 μm , the sorting ranged from 1.29 (well sorted) to 2.33 (poorly sorted), and the dust content ranged from 0.44 to 21.7%. Aishan *et al.*¹⁵ analyzed the grain-size distribution and threshold friction velocities of surface sediments in the landscape of the eastern Tarim Basin. The results reveal significant heterogeneity, with transversal dunes exhibiting the coarsest sediments, while vegetated patches within the Tarim River's alluvial plain are characterized by the finest sediments.

Although there have been many grain-size analyses of sediments in the Taklamakan Desert, most have been limited to certain areas of the desert or certain dune types. Few analyses have been conducted to systematically explore the grain size of sediments with different geomorphologies, regional differentiation patterns, depositional processes, and environments of the entire desert at the macroscopic scale. Therefore, surface sediment samples were systematically collected from a range of modern geomorphic landscapes across the entire Taklamakan Desert, including different dune types, deflation areas, interdune, and other key geomorphic features. These samples were selected to capture regional variations in sediment characteristics, depositional processes, and environmental conditions at a macroscopic scale. Based on these samples, a complete sediment grain size database was constructed. This complete and open-access dataset will provide researchers with basic data for examining the formation and evolution of deserts, sources of sand materials, and the restoration and reconstruction of aeolian environments.

Study Area

The Taklamakan Desert in the central Tarim Basin is the largest sand sea in the mid-latitudes of the Northern Hemisphere, with a width of approximately 500 km, a length of approximately 1,100 km, and an area of roughly 280,000 square kilometers^{4,21,36}. The underlying Quaternary landforms of the Taklamakan Desert are dominated by flooded alluvial fans of rivers under dry climatic conditions, dry deltas, and fluvial-lake-phase plains in certain areas³⁶. Landforms in the Tarim Basin are distributed in a circular pattern, with mountainous landforms on the margins and large oases distributed across mountain-front areas, flood fans, alluvial fans, gravel deserts (Gobi), and sandy deserts from the basin margins to the central part of the basin, in that order³⁷. The Tarim, Yarkant, Aksu, Hotan, Kriya, Niya, and Qarqan rivers develop within the desert, with main water sources of snowmelt and precipitation from the surrounding high mountains (Fig. 1). River runoff is seasonal, with infiltration and evaporation promoting sediment deposition along the river channels. During the dry season, low water levels desiccate the floodplains; river sediments are reprocessed and transported to the desert by the wind³⁸. The mean annual temperature in the basin is 11 °C, annual rainfall ranges between 25 and 40 mm over most of the area, and the annual potential evapotranspiration capacity is between 2,100 and 3,400 mm³⁷.

Over the Tarim Basin, airflow is dominated by a subtropical high-pressure system, whereas at low altitudes, it is controlled by cyclonic and anticyclonic systems³⁹. Two types of winds mainly control the Taklamakan Desert: a northwesterly-westerly circulation from the middle and upper atmospheres and a northeasterly circulation from the lower atmosphere⁴⁰. Northeast winds prevail in the eastern part of the basin near the surface due to the blocking effect of tall mountains, whereas west, northwest, and north winds dominate to the west⁴⁰. Wind acts on loose sediments to form complex and diverse landforms. Sediments from different rivers vary significantly in sediment characteristics owing to the different stratigraphies of their basins³⁶. The main types of sand dunes in the Taklamakan Desert are compound/complex crescent chains, compound dome dunes, and compound/complex linear dunes. In addition to these three composite/complex types, single simple dunes are distributed throughout sand seas⁴¹.

Methods

Stage 1: data acquisition. Sediment sampling sites were deployed along the transportation routes of the Taklamakan Desert. Samples were collected deep in the desert hinterland within roadless areas, covering almost all typical landscapes (Fig. 2). The samples were collected from 2022 to 2024. Figure 1 shows the distribution of the sampling points (596 samples). The samples mainly included 272 mobile dunes, 52 vegetated hummock

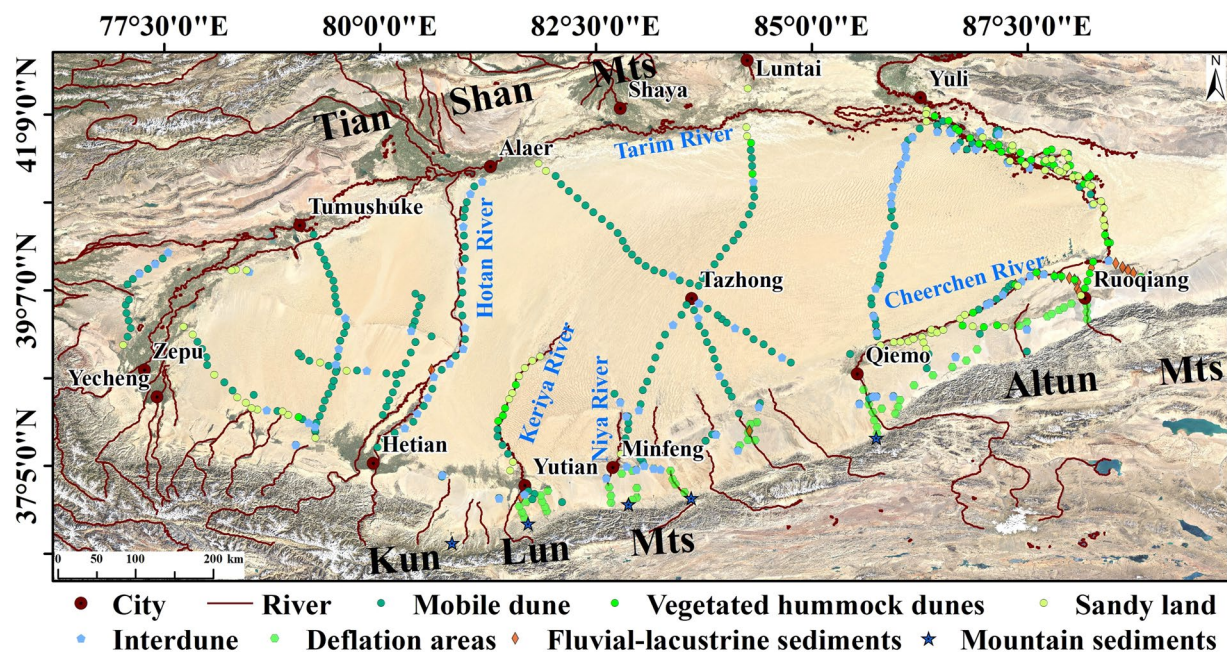


Fig. 1 Map of the study area in the Taklamakan Desert, including sample locations.

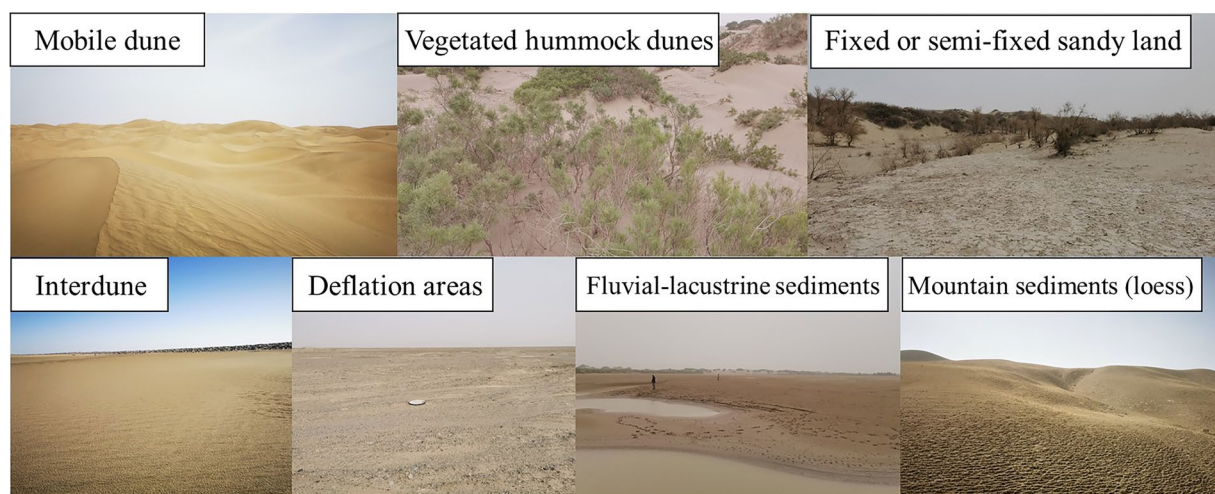


Fig. 2 Seven typical geomorphological landscapes of the Taklamakan Desert.

dunes, 105 interdune sites, 56 deflation areas sites, 32 fluvial-lacustrine sediments, 74 fixed or semi-fixed sandy land sites, and five mountain sediments (loess). The sampling design aimed to capture a comprehensive range of sedimentary environments, focusing on geomorphic features most pertinent to studies of sediment transport, desertification, and environmental change. To improve the representativeness of the samples, an area of approximately 20×20 cm with different geomorphologies was selected to collect sediment samples at depths of 0–10 cm from the surface layer. This depth represents the active zone most directly influenced by modern wind and other dynamic environmental processes. The weight of the samples was approximately 200–1,000 g. Modern deposits are recognized in the field through a combination of distinct geomorphic features, environmental context, and remote sensing imagery. Meanwhile, on-site photographs were taken at each location to record the landscape features surrounding the samples.

Stage 2: Classification of sediment samples. The Taklamakan Desert is characterized by a complex and diverse range of geomorphic types, encompassing nearly all major landform categories. Therefore, the classification of sediment samples is based on the geomorphic context, sedimentary processes, and environmental conditions that govern their formation. The chosen categories reflect key distinctions in how the sediments are deposited and the factors that influence their grain size distribution. These include aeolian processes (wind action), fluvial and lacustrine processes (water action), and the role of vegetation in stabilizing sediments. This

classification aims to identify and describe the different sedimentary environments and the resulting grain size characteristics, allowing for a deeper understanding of the relationships between geomorphology and sediment deposition processes. The main formation process of different types of sediments is as follows:

- (1) Mobile dunes: These are formed by aeolian processes where wind transports and deposits sand grains, creating dynamic, shifting dunes in regions with strong wind activity.
- (2) Vegetated hummock dunes: These dunes are formed by the interaction of wind-driven sand deposition and vegetation, which helps stabilize the sand, leading to the formation of fixed or semi-fixed dune structures typically in areas with lower wind velocities.
- (3) Fixed or semi-fixed sandy land: These areas consist of stabilized or semi-stabilized sand, often due to the presence of vegetation or soil consolidation processes that reduce the mobility of the sand grains, making them less susceptible to wind erosion.
- (4) Interdune: Interdune areas are low-lying regions between dunes where sediment deposition occurs due to a combination of aeolian processes, lacustrine settling, alluvial fan deposits, and loess accumulation, resulting in heterogeneous grain size distributions.
- (5) Deflation areas: Where wind erosion (deflation) removes fine particles, leaving behind coarser materials. These areas are commonly found in arid and semi-arid environments where wind dominates sediment transport.
- (6) Fluvial-lacustrine sediments: These sediments are deposited by fluvial (river) or lacustrine (lake) processes, including those from dried riverbeds, dry lake basins, and floodplains. These environments often feature finer-grained deposits, but coarser materials can also be found in floodplains or deltas.
- (7) Mountain sediments (loess): Mountain sediments, particularly loess, are fine-grained materials deposited by wind in mountainous or hilly regions. These sediments are typically derived from distant sources and are characterized by their fine particle size and susceptibility to wind erosion.

Stage 3: grain size analysis. The sediment grain size was tested using a Mastersizer 3000 laser particle sizer (0.01 to 3,500 μm). Before testing on the machine, gravel larger than 3,500 μm was sieved out to ensure that all particles were within the range of the instrument. The measurements were repeated three times for each sample with a measurement error of less than 2%. Finally, the average of three measurements was used as the particle size distribution data for that sample. Grain size classification was based on the Udden-Wentworth criterion^{42,43}. Particle size parameters were calculated using the Fork-Ward diagrammatic formula⁴⁴. The particle size parameters of the samples were calculated using the GRADISTAT software⁴⁵.

Data Records

The dataset, a comprehensive grain-size database of surface sediments from the Taklamakan Desert⁴⁶, has been uploaded to the Figshare and is available at <https://doi.org/10.6084/m9.figshare.28522457.v1>. It consists of three Excel files: files 1, 2, and 3 describe the grain-size characteristics of sediments from the Taklamakan Desert, with the files 2 and 3 derived from calculations based on the data in file 1.

File 1: Grain Size Database of Sediments from the Taklamakan Desert

Specifically, File 1 contains the following data fields: (1) geomorphic type, including mobile dunes, vegetated hummock dunes, fixed or semi-fixed sandy land, interdune, deflation areas, fluvial-lacustrine sediments, and mountain sediments; (2) latitude and longitude; (3) sample ID; (4) natural frequency of sediments (The volumetric percentage content (%) for each interval within the 0 to 3500 μm range). This file provides fundamental data on the sediment composition across different landscapes, serving as the basis for the subsequent derivation of statistical grain size parameters and particle fractions in Files 2 and 3.

File 2: Grain Size Parameters Database of Sediments from the Taklamakan Desert

The parameters are calculated based on the data in File 1 and are expressed in two formats: micrometers (μm) and phi (ϕ) units. File 2 contains the following data fields: (1) geomorphic type; (2) grain size parameters, the mean grain size, sorting, skewness, and kurtosis were included; (3) sample ID. These indicators can measure the energy of the sediment transport medium and transport mode.

File 3: Particle Fraction Database of Sediments from the Taklamakan Desert

This file provides the content of each sediment sample in terms of its constituent particle fractions. These fractions are calculated based on the grain size components from File 1 and are expressed as volume percentages. File 3 contains the following data fields: (1) geomorphic type; (2) particle fraction; (3) sample ID. This file summarizes the compositional characteristics of the sediments, offering insights into the relative abundance of different particle fractions across various geomorphic units of the Taklamakan Desert.

Probability density of Sediment grain size. Figure 3 shows the grain-size distribution curves and mean grain sizes of different landscapes in the Taklamakan Desert. The mean grain size of the mobile dune had the largest value (164.2 μm), followed by vegetated hummock dunes (125.1 μm) and interdunes (105.3 μm), while the mean grain size of mountain and fluvial-lacustrine sediments reached the minimum, 58.2 and 66.6 μm , respectively. The deflation areas had a mean grain size of 76.6 μm due to eliminating particles larger than 3,500 μm . The mean grain sizes of sediment samples in the Taklamakan Desert (596 samples). From the particle size distribution curve, most particle size distributions for dune sand showed a unimodal distribution; only individual samples showed a bimodal distribution. For other landforms, except for sediment samples from the Kunlun Mountains, such as the interdune, sand land, deflation areas, and fluvial-lacustrine sediments, the particle size distribution

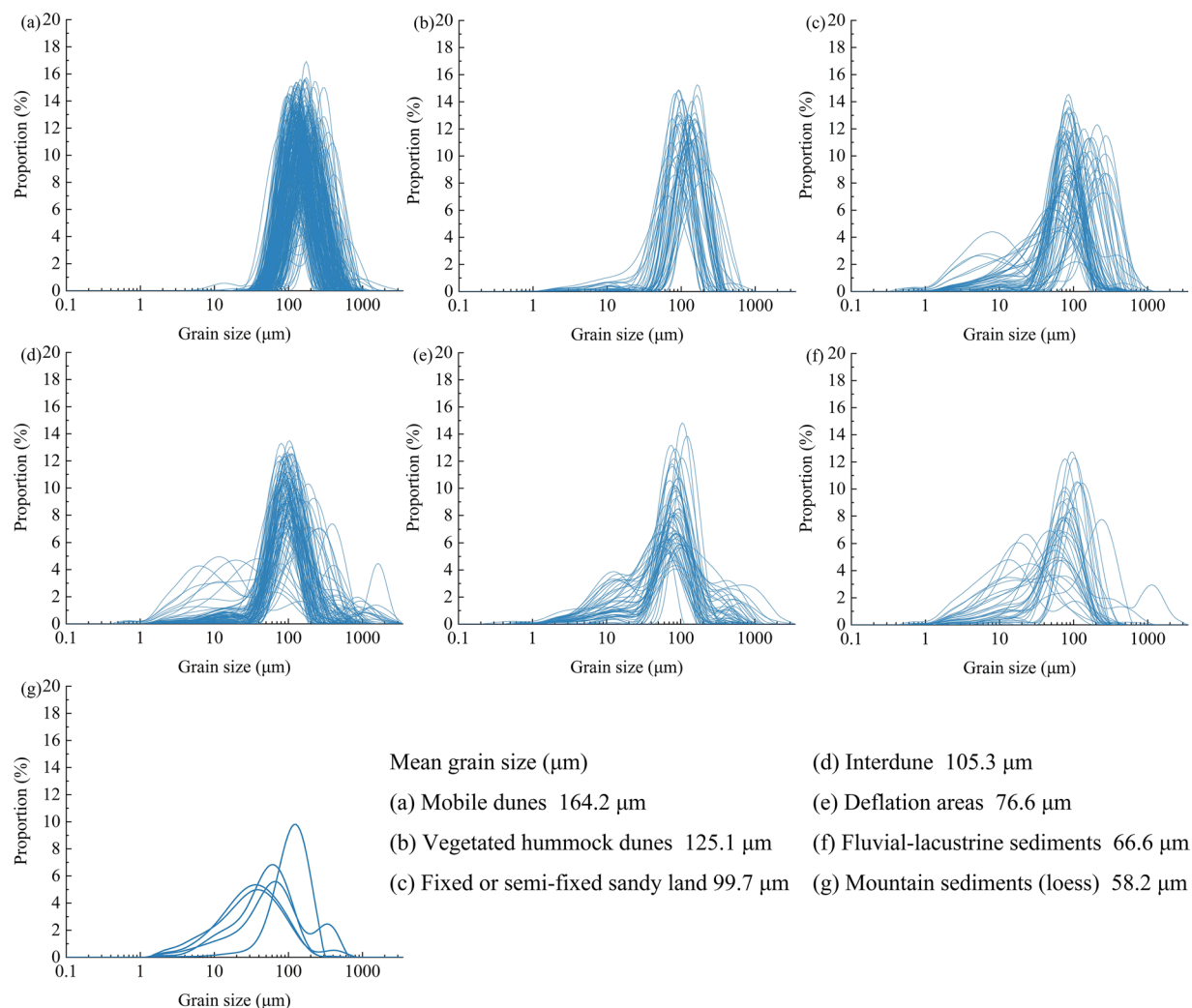


Fig. 3 Grain size frequency distribution curves of different geomorphologies.

was completely different from that of the dune sands. Many samples exhibited bimodal distributions, suggesting complex sediment sources.

Characteristics of sediment grain size parameters. Figure 4a shows that the mean grain size of both the mobile dunes and vegetated hummock dunes in the Taklamakan Desert is primarily composed of fine sand and very fine sand. The mean grain size of the sand samples exhibits considerable variation, predominantly fine sand, very fine sand, and silty clay. For the interdune, except for a few samples where the mean grain size is characterized by silty and clay, the majority consists of fine sand and very fine sand. The mean grain size of the deflation areas and fluvial-lacustrine sediments is mainly composed of very fine sand and silty clay. Figure 4b shows the sorting coefficients of the sediments for each geomorphology. A smaller sorting coefficient value indicates better sorting. Mobile dunes and vegetated hummock dunes have the best sorting, mainly characterized by “well sorted” and “moderately sorted.” This indicates that the sediment particle size of the mobile dunes was relatively uniform. The sorting of other types was relatively poor, where many samples had a sorting coefficient > 1 , belonging to the “poorly sorted” category. These results indicate that different depositional environments significantly control the sorting of sediments. Dune sands have optimal sorting due to the continuous effect of wind. Figure 4c shows the skewness of the sediments for each geomorphology type. A positive skew indicates a relatively higher amount of finer fractions, whereas a negative skew indicates a larger proportion of coarser fractions. As shown in Fig. 4c, most samples had a skewness > -0.1 , which shows near-symmetrical or positive skewness, indicating that fine particles dominate their sediments. A few interdunes showed negative skewness (< -0.1), indicating that these samples had a larger proportion of coarse grains. Figure 4d shows the kurtosis of each geomorphological sediment sample, reflecting the particle size distribution concentration. The higher the kurtosis, the more concentrated the distribution of particles, as well as increased “sharp peak” characteristics. Platykurtic and mesokurtic dunes dominated the mobile dunes, whereas the peaks of other landforms were more dispersed and dominated by mesokurtic and leptokurtic dunes. Overall, Fig. 4 shows the differences in the control of sediment grain size based on the depositional environments of different geomorphologies. The mobile dunes exhibited the best sorting and

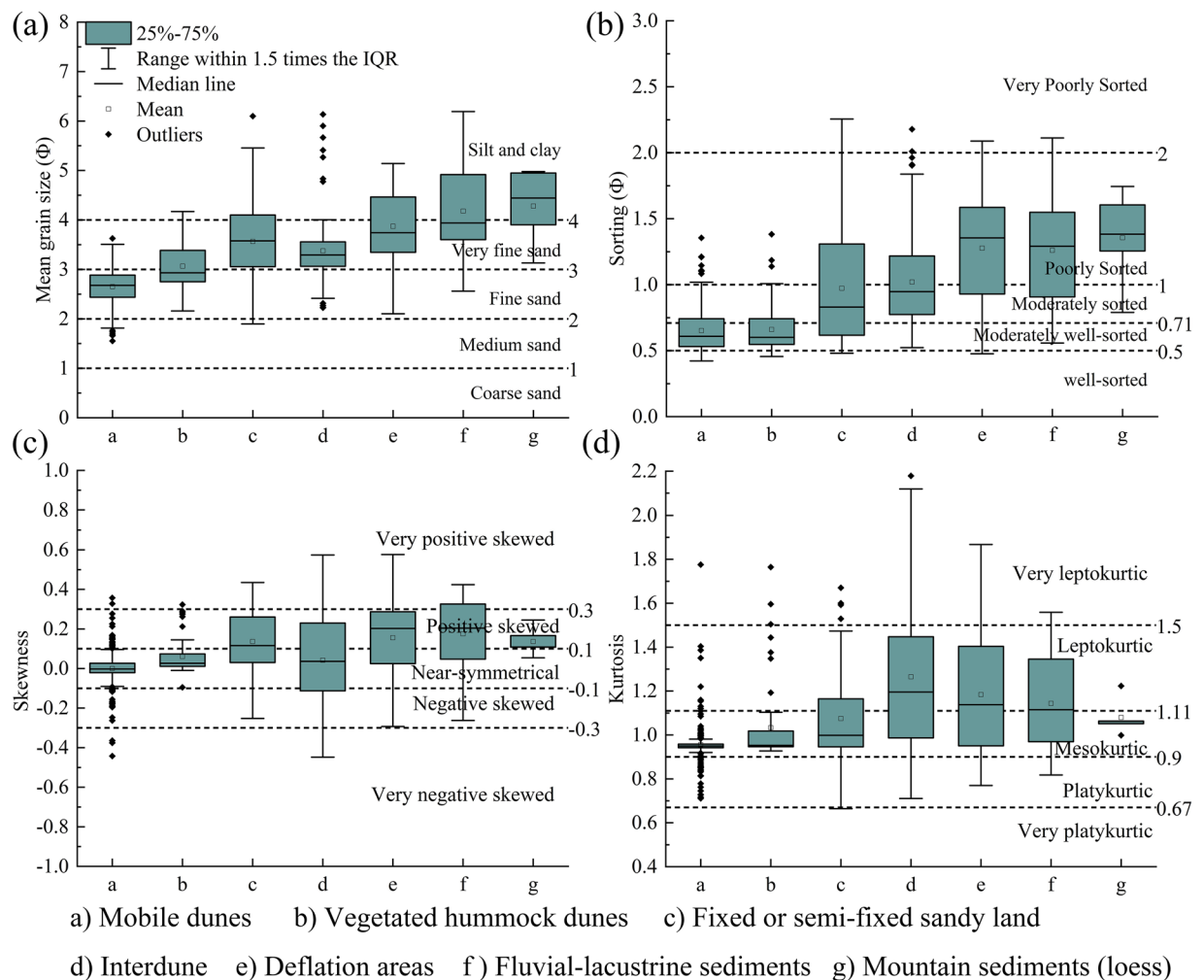


Fig. 4 Grain size parameters of sediments in different geomorphologies. (a) Mean grain size. (b) Sorting. (c) Skewness. (d) Kurtosis.

	Mobile dune	Vegetated hummock dunes	Sandy land	Interdune	Deflation areas	Fluvial-lacustrine sediments	Mountain sediments
Gravel	0.0%	0.0%	0.0%	0.2%	0.0%	0.1%	0.0%
Very coarse sand	0.0%	0.0%	0.0%	0.7%	0.4%	0.4%	0.0%
Coarse sand	1.7%	0.3%	0.8%	1.8%	2.2%	0.6%	0.7%
Medium sand	17.7%	7.3%	7.6%	6.3%	4.1%	2.6%	3.9%
Fine sand	47.2%	40.1%	24.2%	27.1%	16.6%	16.3%	14.7%
Very fine sand	30.6%	41.6%	38.7%	41.8%	38.1%	33.2%	27.1%
Silt and clay	2.9%	10.8%	28.6%	22.0%	38.6%	46.8%	53.6%

Table 1. Sediment particle composition of different geomorphologies.

kurtosis, with more homogeneous and concentrated particles. At the same time, interdune, deflation areas, and fluvial-lacustrine sediments had poorer sorting. The skewness and kurtosis indicate that their sediment particle distributions were more complex and diverse.

Particle fractions of different geomorphologies. Regarding the grain size composition (Table 1), the dominant fractions of dune sands in the Taklamakan Desert were medium, fine, and very fine sands, accounting for 17.7, 47.2, and 30.6%, respectively. Vegetated hummock dunes were finer than the mobile dunes, and their dominant fractions were fine sand (40.1%), very fine sand (41.6%), and silt and clay (10.8%). The dominant fractions of the other geomorphologies, such as the interdune, were fine sand, very fine sand, and silt-clay, accounting for 27.1, 41.8, and 22%, respectively.

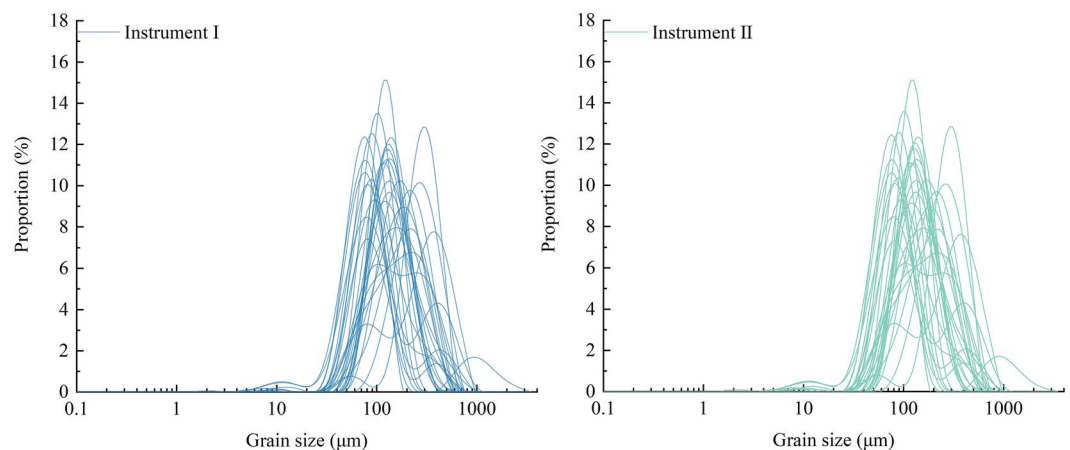


Fig. 5 Grain size frequency distribution curves from different instruments.

Technical Validation

The sediment grain size dataset from the Taklamakan Desert has undergone rigorous validation procedures to ensure its accuracy, reliability, and representativeness. A series of technical steps were carefully implemented throughout the data collection, processing, and analysis stages to guarantee the high quality and reproducibility of the results.

Grain size measurement and instrumentation. The sediment grain size was measured using high-precision laser diffraction particle size analyzers (Mastersizer 3000), which allows for accurate sediment analysis ranging from fine silt and clay to coarser gravel (0.01–3500 μm). To ensure reliable measurements, we thoroughly cleaned the instruments with water twice before measuring each sample to prevent any cross-contamination that could affect the results of subsequent samples. Additionally, three sets of duplicate samples were analyzed at each site to assess the precision and consistency of the results.

Data quality control and error minimization. To minimize potential errors, sediment samples underwent repeated measurements at the laboratory. A subset of these samples, totaling thirty, was also sent to an independent laboratory for verification of the grain size distributions. As shown in Fig. 5 (grain size frequency distribution curves) and Table 2 (comparison of grain size parameters), the correlation between the results from both laboratories was strong, confirming the accuracy and robustness of the data. Specifically, the comparison of grain size characteristics between the two laboratories demonstrated reliable consistency. Furthermore, the particle size distribution data were carefully checked for outliers. If the measurements of a sample showed significant discrepancies between the repeated tests, the sample was re-measured to ensure reliability. This process ensured that the dataset is free from systematic errors and that all data points are accurate and dependable.

Data documentation and transparency. Comprehensive metadata is provided for each data point to facilitate transparency and reproducibility. This metadata includes information such as the sampling location, depth, and measurement technique. Detailed descriptions of all methods, protocols, and calibration procedures are included in the dataset documentation. This enables other researchers to replicate the analysis or apply similar methods in other desert regions or environments.

Usage Notes

Thanks to transportation and logistical access advancements, we conducted this large-scale sampling effort, providing one of the most comprehensive grain size datasets for the Taklamakan Desert. The dataset includes detailed measurements of sediment characteristics from several typical geomorphic units within the desert. Although the Taklamakan Desert is known for its complex and diverse geomorphologies, we focused our sampling efforts on the most representative and common landscapes. As a result, this dataset does not cover all geomorphic types found in the desert. Instead, it provides an in-depth analysis of those most relevant to sediment transport, desertification, and environmental evolution studies. As a result, the dataset provides a detailed, though geographically limited, representation of sediment characteristics.

Data interpretation and limitations. **Grain Size and Sampling Depth:** All sediment samples in this dataset were collected from the desert's 0–10 cm surface layer. During the grain size measurement process, particles larger than 3500 μm were excluded, as they exceeded the measurement range of the equipment. While this ensures an accurate representation of finer sediments (sand, silt, clay), it should be noted that the exclusion of gravel particles may significantly impact the characterization of deflation areas sediments, which typically contain larger grains.

Instrument I				Instrument II			
Mean grain size	Sorting	Skewness	Kurtosis	Mean grain size	Sorting	Skewness	Kurtosis
$M_z(\varphi)$	$\sigma_1(\varphi)$	Sk_i	K_G	$M_z(\varphi)$	$\sigma_1(\varphi)$	Sk_i	K_G
1.765	0.615	0.165	1.130	1.770	0.622	0.175	1.155
2.650	0.838	0.026	0.899	2.648	0.842	0.026	0.898
2.290	0.764	0.122	1.007	2.309	0.773	0.125	1.008
2.554	0.936	0.156	0.900	2.565	0.936	0.155	0.895
3.632	0.572	0.001	0.955	3.642	0.569	0.011	0.956
2.502	0.791	0.080	0.943	2.510	0.790	0.081	0.942
3.513	0.852	−0.214	1.397	3.512	0.859	−0.218	1.409
3.194	0.521	−0.011	0.956	3.201	0.519	−0.010	0.954
3.189	0.989	−0.339	1.329	3.204	0.974	−0.330	1.323
2.433	0.684	−0.014	0.941	2.439	0.681	−0.012	0.940
2.555	1.012	−0.023	0.813	2.564	1.012	−0.024	0.813
2.749	0.790	−0.109	0.963	2.752	0.800	−0.111	0.963
2.773	0.692	−0.027	0.956	2.776	0.689	−0.024	0.952
2.800	0.587	−0.033	0.950	2.807	0.586	−0.033	0.951
2.760	0.570	0.002	0.950	2.758	0.570	0.002	0.950
2.688	1.254	−0.310	0.723	2.690	1.262	−0.300	0.726
3.216	1.146	−0.363	1.942	3.230	1.122	−0.351	1.922
3.063	0.846	−0.163	1.037	3.064	0.846	−0.162	1.037
2.053	1.209	0.328	0.838	2.077	1.232	0.327	0.828
2.822	0.604	−0.033	0.958	2.825	0.603	−0.032	0.958
3.736	0.673	0.136	1.047	3.741	0.676	0.140	1.054
2.811	0.639	−0.059	0.967	2.807	0.649	−0.062	0.966
2.789	0.621	0.002	0.945	2.787	0.625	−0.001	0.947
1.896	0.692	0.052	0.943	1.925	0.697	0.049	0.942
3.375	0.559	−0.012	0.947	3.379	0.558	−0.010	0.946
2.520	0.971	0.063	0.856	2.523	0.975	0.060	0.857
3.383	1.027	−0.116	1.214	3.402	1.029	−0.098	1.231
2.936	0.468	−0.005	0.960	2.935	0.469	−0.005	0.960
2.961	0.635	−0.022	0.949	2.958	0.636	−0.021	0.949
2.567	0.802	−0.166	1.020	2.565	0.808	−0.173	1.023

Table 2. Comparison of grain size parameter results measured by different instruments.

Data availability

Sample Availability: All sediment samples included in this dataset have been preserved for potential future studies. Researchers wishing to access the physical samples or conduct additional analyses can request them directly from the authors, subject to academic use and logistical arrangements.

Code availability

No specific code was used to crease or process the sediment grain size dataset from the Taklamakan Desert.

Received: 10 December 2024; Accepted: 31 March 2025;
Published online: 07 April 2025

References

1. Mbow, H.-O. P., Reisinger, A., Canadell, J. & O'Brien, P. Special Report on climate change, desertification, land degradation, sustainable land management, food security, and greenhouse gas fluxes in terrestrial ecosystems (SR2). *Ginevra, IPCC* **650**, (2017).

2. Goudie, A. *Great Warm Deserts of the World: Landscapes and Evolution*. vol. 1 (Oxford University Press, 2002).

3. Williams, M. *Climate Change in Deserts*. (Cambridge University Press, 2014).

4. Xiaoping, Y. & Eitel, B. Understanding the interactions between climate change, landscape evolution, surface processes and tectonics in the Earth System: What can the studies of Chinese deserts contribute? *Acta Geologica Sinica-English Edition* **90**, 1444–1454 (2016).

5. Liu, B. *et al.* Grain-size study of aeolian sediments found east of Kumtagh Desert. *Aeolian Research* **13**, 1–6 (2014).

6. Livingstone, I. Grain-size variation on a 'complex'linear dune in the Namib Desert. *Geological Society, London, Special Publications* **35**, 281–291 (1987).

7. Wang, X., Dong, Z., Zhang, J., Qu, J. & Zhao, A. Grain size characteristics of dune sands in the central Taklimakan Sand Sea. *Sedimentary Geology* **161**, 1–14 (2003).

8. Anderson, J. L. & Walker, I. J. Airflow and sand transport variations within a backshore–parabolic dune plain complex: NE Graham Island, British Columbia, Canada. *Geomorphology* **77**, 17–34 (2006).

9. Purkait, B. The use of grain-size distribution patterns to elucidate aeolian processes on a transverse dune of Thar Desert, India. *Earth Surface Processes and Landforms. The Journal of the British Geomorphological Research Group* **35**, 525–530 (2010).
10. Langford, R. P., Gill, T. E. & Jones, S. B. Transport and mixing of eolian sand from local sources resulting in variations in grain size in a gypsum dune field, White Sands, New Mexico, USA. *Sedimentary Geology* **333**, 184–197 (2016).
11. Wei, G. *et al.* Grain-size composition of the surface sediments in Chinese deserts and the associated dust emission. *Catena* **219**, 106615 (2022).
12. An, Z. The history and variability of the East Asian paleomonsoon climate. *Quaternary Science Reviews* **19**, 171–187 (2000).
13. Singh, C. K., Kumar, P., Kumar, A. & Mukherjee, S. Depositional environment in great Indian desert using grain size parameters and its chemical characterization. *Journal of the Geological Society of India* **86**, 412–420 (2015).
14. Thompson, N. & Caissie, B. E. Evaluating the paleoenvironmental significance of sediment grain size in Bering Sea sediments during Marine Isotope Stage 11. *Stratigraphy* **19**, (2022).
15. Aishan, T. *et al.* Grain size characteristics of a degraded Tugai riparian forest landscape between Taklamakan and Kuruktagh deserts in the eastern Tarim Basin, northwest China. *International Journal of Sediment Research* **39**, 531–539 (2024).
16. Shepard, F. P. Nomenclature based on sand-silt-clay ratios. *Journal of sedimentary Research* **24**, 151–158 (1954).
17. Kirby, M. E. *et al.* Evidence for insolation and Pacific forcing of late glacial through Holocene climate in the Central Mojave Desert (Silver Lake, CA). *Quaternary Research* **84**, 174–186 (2015).
18. Weltje, G. J. & Prins, M. A. Genetically meaningful decomposition of grain-size distributions. *sedimentary geology* **202**, 409–424 (2007).
19. Dietze, E. *et al.* Sediment transport processes across the Tibetan Plateau inferred from robust grain-size end members in lake sediments. *Climate of the Past* **10**, 91–106 (2014).
20. Wang, Y., He, Y., Zhan, J. & Li, Z. Identification of soil particle size distribution in different sedimentary environments at river basin scale by fractal dimension. *Scientific Reports* **12**, 10960 (2022).
21. Jiang, Q. & Yang, X. Sedimentological and geochemical composition of aeolian sediments in the Taklamakan Desert: Implications for provenance and sediment supply mechanisms. *Journal of Geophysical Research: Earth Surface* **124**, 1217–1237 (2019).
22. Shao, T., Zhao, J. & Dong, Z. Grain-size distribution of the aeolian sediment and its effect on the formation and growth of mega-dunes in the Badain Fijaran Desert, north-west China. *Z für Geomorphologie* **59**, 273–286 (2015).
23. Liang, A. *et al.* Provenance and transport process for interdune sands in the Kumtagh Sand Sea, Northwest China. *Geomorphology* **367**, 107310 (2020).
24. Lancaster, N. Grain size characteristics of Namib Desert linear dunes. *Sedimentology* **28**, 115–122 (1981).
25. Lancaster, N. Grain-size characteristics of linear dunes in the southwestern Kalahari. *Journal of Sedimentary Research* **56**, 395–400 (1986).
26. Kasper-Zubillaga, J. J. & Carranza-Edwards, A. Grain size discrimination between sands of desert and coastal dunes from northwestern Mexico. *Revista Mexicana de Ciencias Geológicas* **22**, 383–390 (2005).
27. Zhang, Z., Dong, Z. & Li, J. Grain-size characteristics of dune networks in china's tengger desert. *Geografiska Annaler: Series A, Physical Geography* **97**, 681–693 (2015).
28. Tsoar, H. GrainSize Characteristics of on a Desert Seif. in *Geography Research Forum* vol. 10 37–50 (1990).
29. Gao, X., Narteau, C. & Rozier, O. Controls on and effects of armoring and vertical sorting in aeolian dune fields: A numerical simulation study. *Geophysical Research Letters* **43**, 2614–2622 (2016).
30. van Ijendoorn, C., Hallin, C., Reniers, A. & de Vries, S. Modeling Multi-Fraction Coastal Aeolian Sediment Transport With Horizontal and Vertical Grain-Size Variability. *Journal of Geophysical Research: Earth Surface* **128**, e2023JF007155 (2023).
31. Ferrat, M. *et al.* Improved provenance tracing of Asian dust sources using rare earth elements and selected trace elements for palaeomonsoon studies on the eastern Tibetan Plateau. *Geochimica et Cosmochimica Acta* **75**, 6374–6399 (2011).
32. Huo, W. *et al.* Observed particle sizes and fluxes of Aeolian sediment in the near surface layer during sand-dust storms in the Taklamakan Desert. *Theoretical and Applied Climatology* **130**, 735–746 (2017).
33. Yang, X. *et al.* Estimation of sampling efficiency of the Big Spring Number Eight (BSNE) sampler at different heights based on sand particle size in the Taklimakan Desert. *Geomorphology* **322**, 89–96 (2018).
34. Chen, X. *et al.* Provenance of sub-aerial surface sediments in the Tarim Basin, Western China. *Catena* **198**, 105014 (2021).
35. Zhou, Y., Yang, X., Zhang, D., Mackenzie, L. L. & Chen, B. Sedimentological and geochemical characteristics of sediments and their potential correlations to the processes of desertification along the Keriya River in the Taklamakan Desert, western China. *Geomorphology* **375**, 107560 (2021).
36. Zhu, Z. *et al.* *Study on the Geomorphology of Wind-Drift Sands in the Taklamakan Desert*. Beijing: Science Press, (in Chinese) (1981).
37. Zhu, B. *et al.* Formation and evolution of sand deserts in Xinjiang, Northwest China: I. Provenances of desert sands. *Journal of Geographical Sciences* **24**, 177–190 (2014).
38. Langford, R. P. Fluvial-aeolian interactions: Part I, modern systems. *Sedimentology* **36**, 1023–1035 (1989).
39. Yang, X., Zhu, Z., Jaekel, D., Owen, L. & Han, J. Late Quaternary palaeoenvironment change and landscape evolution along the Keriya River, Xinjiang, China: the relationship between high mountain glaciation and landscape evolution in foreland desert regions. *Quaternary International* **97**, 155–166 (2002).
40. Zu, R. *et al.* Characteristics of near-surface wind regimes in the Taklimakan Desert, China. *Geomorphology* **96**, 39–47 (2008).
41. Wang, X., Dong, Z., Zhang, J. & Chen, G. Geomorphology of sand dunes in the Northeast Taklimakan Desert. *Geomorphology* **42**, 183–195 (2002).
42. Udden, J. A. Mechanical composition of clastic sediments. *Bulletin of the geological society of America* **25**, 655–744 (1914).
43. Wentworth, C. K. A scale of grade and class terms for clastic sediments. *The journal of geology* **30**, 377–392 (1922).
44. Folk, R. L. & Ward, W. C. Brazos River bar [Texas]; a study in the significance of grain size parameters. *Journal of sedimentary research* **27**, 3–26 (1957).
45. Blott, S. J. & Pye, K. GRADISTAT: a grain size distribution and statistics package for the analysis of unconsolidated sediments. *Earth surface processes and Landforms* **26**, 1237–1248 (2001).
46. Li, H. *et al.* A comprehensive grain-size database of surface sediments from the Taklamakan Desert. *figshare* <https://doi.org/10.6084/m9.figshare.28522457.v1> (2025).

Acknowledgements

This study was supported by the Third Xinjiang Scientific Expedition and Research Program-Investigation and Risk Assessment of Drought and Aeolian Disasters in Tarim River Basin (No. 2021xjkk0300), Xinjiang Tianshan Talent Program (No. 2022TSYCLJ0002), the Major Science and Technology Special Project of Xinjiang Uygur Autonomous Region - Research and Application of the Key Technologies for the Construction of Forest and Grass Belt at the Desert's Edge (No. 2024A03009-1), and the Basic Frontier Project of Xinjiang Institute of Ecology and Geography, Chinese Academy of Sciences (No. E3500201).

Author contributions

H.L., X.G. and Y.Z. conceived the idea. H.L. and X.G. created and populated the database with contributions from all coauthors. H.L., J.Z., Z.H., Z.C. and Z.Y. performed the experiment. H.L. and X.G. performed the analysis and wrote the first draft. X.G. and S.L. coordinated the work and reviewed the manuscript. S.L., Y.Z. and X.G. assisted with quality control and reviewed the manuscript. All co-authors read and revised drafts of the manuscript.

Competing interests

The authors declare that they have no known competing financial interests or personal relationships that could have appeared to influence the work reported in this paper.

Additional information

Correspondence and requests for materials should be addressed to X.G.

Reprints and permissions information is available at www.nature.com/reprints.

Publisher's note Springer Nature remains neutral with regard to jurisdictional claims in published maps and institutional affiliations.



Open Access This article is licensed under a Creative Commons Attribution-NonCommercial-NoDerivatives 4.0 International License, which permits any non-commercial use, sharing, distribution and reproduction in any medium or format, as long as you give appropriate credit to the original author(s) and the source, provide a link to the Creative Commons licence, and indicate if you modified the licensed material. You do not have permission under this licence to share adapted material derived from this article or parts of it. The images or other third party material in this article are included in the article's Creative Commons licence, unless indicated otherwise in a credit line to the material. If material is not included in the article's Creative Commons licence and your intended use is not permitted by statutory regulation or exceeds the permitted use, you will need to obtain permission directly from the copyright holder. To view a copy of this licence, visit <http://creativecommons.org/licenses/by-nc-nd/4.0/>.

© The Author(s) 2025